

UIFV: Data Reconstruction Attack in Vertical Federated Learning

Jirui Yang^a, Peng Chen^a, Zhihui Lu^{a,b}, Qiang Duan^d and Yubing Bao^a

^aSchool of Computer Science, Fudan University, Shanghai, 200433, China

^bShanghai Blockchain Engineering Research Center, Shanghai, 200433, China

^cInstitute of Financial Technology, Fudan University, Shanghai, 200433, China

^dInformation Sciences & Technology, Pennsylvania State University, PA, 16802, USA

ARTICLE INFO

Keywords:

Vertical federated learning, privacy risks, data leakage, Unified InverNet Framework (UIFV), data reconstruction, intermediate feature data.

ABSTRACT

Vertical Federated Learning (VFL) facilitates collaborative machine learning without the need for participants to share raw private data. However, recent studies have revealed privacy risks where adversaries might reconstruct sensitive features through data leakage during the learning process. Although data reconstruction methods based on gradient or model information are somewhat effective, they reveal limitations in VFL application scenarios. This is because these traditional methods heavily rely on specific model structures and/or have strict limitations on application scenarios. To address this, our study introduces the Unified InverNet Framework into VFL, which yields a novel and flexible approach (dubbed UIFV) that leverages intermediate feature data to reconstruct original data, instead of relying on gradients or model details. The intermediate feature data is the feature exchanged by different participants during the inference phase of VFL. Experiments on four datasets demonstrate that our methods significantly outperform state-of-the-art techniques in attack precision. Our work exposes severe privacy vulnerabilities within VFL systems that pose real threats to practical VFL applications and thus confirms the necessity of further enhancing privacy protection in the VFL architecture.

1. Introduction

In the current field of artificial intelligence, Vertical Federated Learning (VFL) is regarded as a significant transformative strategy Chen et al. (2020); Khan et al. (2022); Tan et al. (2022). VFL allows different institutions to collaborate on model training while protecting their respective data privacy. This approach is particularly applicable in scenarios where different institutions hold different feature data of the same set of users, such as in the finance and healthcare sectors Li et al. (2019); Lu et al. (2020). The participants in a VFL framework consist of an active party and some passive parties Kang et al. (2022). Each passive party owns a set of data features that are fed into a model (called a bottom model) for local training. The active party holds the label information and a top model in addition to its own feature set and bottom model. The active party coordinates the training process by concatenating the bottom model outputs as the input to the top model. This structure enables collaborative model training without the need to share original data, thus preserving the privacy of sensitive data on the participants.

Despite the advantages of VFL in protecting private data, recent studies have shown that it may still face risks of data privacy breaches Geiping et al. (2020); Wu et al. (2022), especially through data reconstruction attacks. Such attacks reconstruct the original features of the training dataset by analyzing intermediate data during the VFL process, potentially leading to sensitive information leaks.

***Corresponding author: Zhihui Lu

✉ yangjr23@m.fudan.edu.cn (J. Yang); pengchen20@fudan.edu.cn (P. Chen); lzh@fudan.edu.cn (Z. Lu); qduan@psu.edu (Q. Duan); ybbao23@m.fudan.edu.cn (Y. Bao)

ORCID(s):

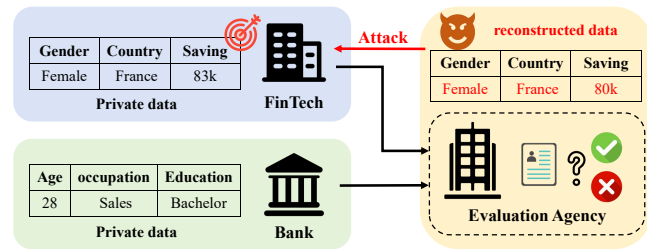


Figure 1: Illustration of a VFL data reconstruction attack, showing the bank and Fintech company with their bottom models and the evaluation agency with the top model and a bottom model. The agency conducts an attack on the FinTech company's model using VFL intermediate data to access private data while adhering to VFL protocols.

Figure 1 shows a VFL application scenario that is vulnerable to data reconstruction attacks Chen et al. (2022). In this scenario, a bank and a fintech company participate in a VFL for credit analysis, with each entity possessing a subset of user attributes. An assessment agency uses the labels of users to coordinate the training of the VFL model. However, the assessment agency wants to acquire the fintech company's private data and take it for its own use, so it launches a data reconstruction attack on the model owned by the fintech company. Without violating the VFL protocol, it uses the intermediate data from the VFL to reconstruct the private data owned by the bank, leading to the leakage of the fintech company's customer information and posing a significant security risk to the actual application of VFL.

Existing data reconstruction attacks on VFL, such as the generative regression network (GRN) method Luo et al. (2021) and the gradient-based inversion attack (GIA) method Jiang et al. (2022), largely draw from methods used in HFL

(Horizontal Federated Learning), with a core focus on utilizing model information. However, these methods have certain limitations. For instance, the GRN method is designed for a white-box attack scenario where the reconstruction process requires access to the passive party’s model, which significantly restricts its applicability. Although the GIA method enables a black-box attack, it imposes very strict requirements on the model, demanding a logistic regression model and forbids non-linear activation functions in the output layer of neural networks, which also greatly limits the method’s applicability.

To gain a more thorough understanding of the potential threats to data privacy in VFL, it is crucial to go beyond the existing attack methods and explore a broader range of attack scenarios. The goal of this paper is to fully consider real-world attack scenarios in practical VFL environments and develop effective attack methods for different scenarios. To accomplish this, we have completely abandoned the traditional approach that relies on gradient information or model information and instead have opted to directly utilize the intermediate feature data generated in the VFL framework for attacks. This method constructs an inverse net (InverNet) to effectively extract original data information from the intermediate features output from the target’s model. Following this strategy, We have developed an innovative attack framework, called Unified InverNet Framework in VFL (UIFV), that is applicable to a variety of VFL scenarios with different adversary capabilities. UIFV overcomes the dependency on gradient information or model information of traditional attacks in VFL, thereby providing a more flexible and effective means for data reconstruction attacks in complex VFL environments.

Specifically, we make the following contributions in this paper.

- **Innovative Attack Method:** We propose a new type of VFL data reconstruction attack method that does not rely on gradient information or model information but leverages the intermediate features output from the target’s model through an InverNet to reconstruct original data.
- **Flexible Attack Framework:** We develop a framework UIFV that is applicable in various black-box attack scenarios for effective data reconstruction in VFL with different adversary’s capabilities.
- **Stealth and Non-Intrusiveness:** The method and framework are designed to be stealthy and non-intrusive, allowing attacks without disrupting normal VFL operations and less likely to be detected.
- **High Attack Effectiveness:** We have conducted extensive experiments to evaluate the effectiveness of the proposed method and verified its higher attack accuracy compared to state-of-the-art methods.

The remainder of this paper is organized as follows: Section 2 briefly reviews related works on Vertical Federated

Learning (VFL) and associated attacks. Section 3 defines the problem. In Section 4, we provide an overview of the UIFV attack framework. Section 5 details the four scenarios within the UIFV attack framework. Section 6 presents experimental results of UIFV in VFL, demonstrating the success of our attack. Finally, the paper is concluded with a summary in Section 7.

2. Related Work

2.1. Vertical Federated Learning

Within the framework of federated learning, based on the distribution characteristics of local data, it is mainly divided into two scenarios: Horizontal Federated Learning (HFL) and Vertical Federated Learning (VFL). In HFL Li et al. (2021a,b); Zhuang et al. (2021), the local datasets of data owners have almost no intersection in the sample space, but there is a significant overlap in the feature space. In contrast, in VFL Chen et al. (2020); Khan et al. (2022); Tan et al. (2022), local datasets have a large intersection in the sample space, but little overlap in the feature space. Each of these federated learning types has its applicable scenarios and advantages. VFL is particularly suitable for situations where different institutions hold different feature data of the same set of users; for example, in the financial sector, one institution may have the credit history of users, while another may have their transaction data. Through VFL, these institutions can collaborate to build more accurate risk assessment models without the need to directly exchange sensitive data. VFL has found wide applications in fields such as finance and healthcare Li et al. (2022); Wei et al. (2023).

The participants in a VFL framework consist of an active party and some passive parties Kang et al. (2022). Each passive party owns a set of data features that are fed into a model (called a bottom model) for local training. The active party holds the label information and a top model in addition to its own feature set and bottom model. The active party coordinates the training process by concatenating the bottom model outputs as the input to the top model. This structure enables collaborative model training without the need to share original data, thus preserving the privacy of sensitive data on the participants.

2.2. Data Reconstruction Attack

Current data reconstruction research can be categorized into gradient-based, model information-based, and feature-based methods.

Gradient-based methods use gradients generated during machine learning model training for data reconstruction. Beginning with the seminal work Zhu et al. (2019), a substantial body of research, including Geiping et al. (2020) and Zhao et al. (2020), has utilized gradient data for reconstruction, achieving significant empirical results. Vero et al. (2022) introduced TabLeak, a novel method for tabular data, while Pan et al. (2022) investigated the security boundaries of gradient data reconstruction. However, these methods, mainly

applicable to HFL architecture, face challenges in VFL architecture where accessing gradient information is difficult. Jin et al. (2021) considered a VFL scenario with shared parameters among underlying models, enabling direct data reconstruction via gradients, but this is not universally applicable in VFL.

Model information-based reconstruction methods use the internal parameters of machine learning models to reconstruct original training data. Luo et al. (2021) proposed the GRN method for recovering data of the passive party in VFL, requiring access to the passive party’s model and its parameters. Jiang et al. (2022) improved the GRN method and proposed GIA, which constructs a shadow model using a small amount of known auxiliary data and their confidence scores, emulating the real passive party’s model for data reconstruction without direct access. Essentially, this approach still relies on utilizing the model’s internal parameters, employing a white-box method for data reconstruction. However, obtaining the passive party’s model in VFL architecture is difficult due to participants’ concerns over data privacy and security, often making them reluctant to share their model details.

Feature-based methods reconstruct data using outputs like Shapley values or intermediate features. In traditional machine learning, Luo et al. (2022) first revealed the risks of feature inference attacks in model explanations based on Shapley values, demonstrating that current explanation methods are prone to privacy leaks. In split learning, He et al. (2019) and He et al. (2020) studied data privacy leakage, and Yin et al. (2023) introduced the Gincer attack, confirming the severity of privacy issues in such systems. Pasquini et al. (2021) explored the risks of malicious servers in learning processes. Despite numerous studies in this area, specific methods for VFL architecture are lacking. Our method reconstructs data using intermediate features of the VFL passive party’s model, treating it as a black-box, significantly broadening the application scenarios and enhancing the flexibility and applicability of VFL data reconstruction attacks.

3. Preliminaries

3.1. System Model

Without loss of generality, we consider a VFL system with K participants, $\mathbb{P}_1, \dots, \mathbb{P}_K$, where $K \geq 2$. Each sample $x_i = \{x_i^1, \dots, x_i^K\}$ is a vector that comprises K sets of features each owned by one participant; i.e., x_i^k is the feature set provided by participant \mathbb{P}_k . The label set $\{y_i\}_{i=1}^N$ can be viewed as a special feature that is typically owned by one of the participants, say \mathbb{P}_1 , which is referred to as the active party, while the other participants are called passive parties.

The VFL model can be represented as $f_{\text{top}}(H^1, \dots, H^K)$, where $H^k = f_k(\theta_k; x^k)$. $f_{\text{top}}()$ is the top model controlled by the active party (owner of the labeled data), and $f_k(\theta_k; x^k)$ ($k = 1, \dots, K$) are the bottom models of the K participants. For training the entire model, each participant \mathbb{P}_k feeds the bottom model $f_k(\theta_k; x^k)$ with its own feature set $x_i^k, i = 1, \dots, N$ to generate the intermediate features H^k , which is

Setting	i.i.d. Data	Inference Query	Minimal x^{target}
Query Attack	✓	✓	-
Data Passive Attack	✓	-	-
Isolated Query Attack	-	✓	-
Stealth Attack	-	-	✓

Table 1

Adversary’s capability in our consideration (✓: the adversary possess this capability; -: this capability is not necessary.)

then sent to the active party. The active party concatenates the intermediate features received from all participants to form the input to the top model and completes the forward propagation to generate an output, which is then used together with the label to calculate the loss function and determine the gradients. The top model is first updated based on the gradients, and then the partial gradients with respect to each bottom model are sent back to the participants to complete the backpropagation and update the bottom models. Therefore, the VFL model training can be formulated as

$$\min_{\Theta} \mathbb{E}_{(x,y) \sim \mathcal{D}} \mathcal{L}(f_{\text{top}}(H^1, \dots, H^K), y), \quad (1)$$

where \mathcal{D} is the training dataset, \mathcal{L} is the loss function, and $\Theta = \{\theta_1, \dots, \theta_K; \theta_{\text{top}}\}$ are VFL model parameters.

3.2. Threat Model

In this study, we assume that the adversary \mathbb{P}_{adv} is the active party. One of the passive parties is the target of the attack, denoted as $\mathbb{P}_{\text{target}}$. All participants strictly adhere to the VFL protocol.

Adversary’s objective. The goal of the attack is to acquire the private data x^{target} used by $\mathbb{P}_{\text{target}}$ in VFL training. This objective is quite ambitious, fundamentally challenging privacy preservation in VFL. Naturally, this is also very difficult to achieve, and nearly impossible in some practical scenarios. Therefore, the goal of the attack may be reduced to acquiring as much information about x^{target} as possible, for example obtaining information about a specific column in x^{target} .

Adversary’s capacity. We assume that the attacker \mathbb{P}_{adv} strictly follows the VFL protocol and cannot disrupt the normal operations on $\mathbb{P}_{\text{target}}$; therefore, \mathbb{P}_{adv} has no access to the bottom model at $\mathbb{P}_{\text{target}}$. Since \mathbb{P}_{adv} is on the active party, it can obtain the intermediate features H^1, \dots, H^K from all participants including $\mathbb{P}_{\text{target}}$. In different VFL scenarios, \mathbb{P}_{adv} may have the following capabilities: possesses an auxiliary dataset with an identical and independent distribution (i.i.d.) as x^{target} , make inference queries to the $\mathbb{P}_{\text{target}}$ ’s model, or obtain a minimal amount of private data samples used by $\mathbb{P}_{\text{target}}$ for local training.

The adversary may launch a variety of attacks for data reconstruction based on the different capabilities that it has. Table 1 lists the attack scenarios and the required adversary capabilities. In the Query Attack scenario, the attacker possesses an i.i.d. auxiliary dataset and can make queries to

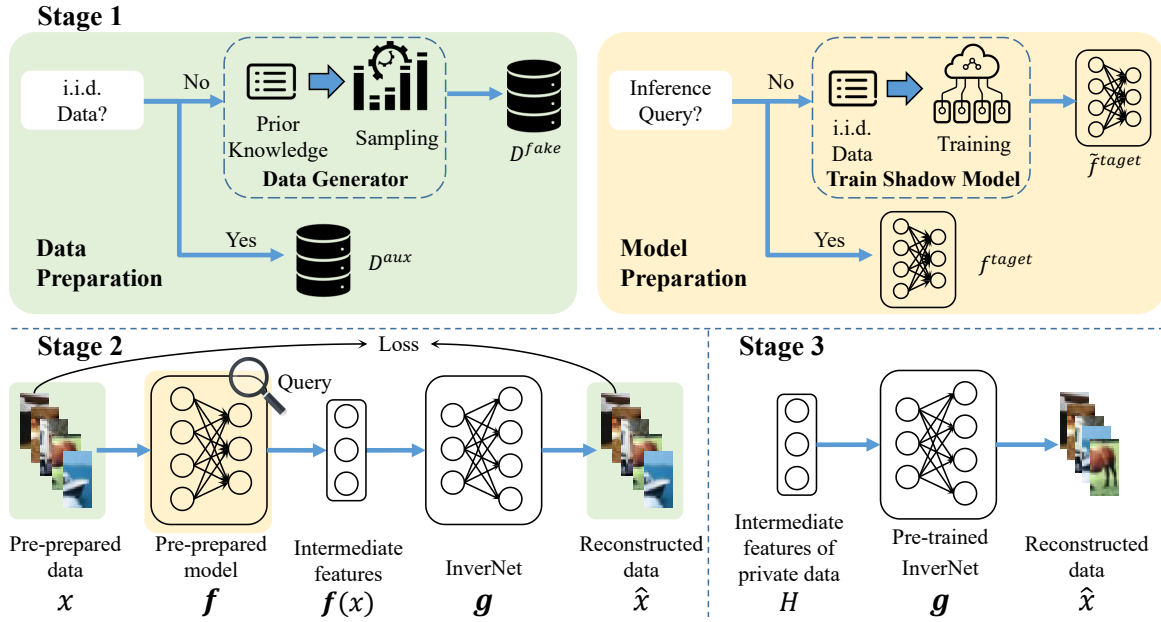


Figure 2: An overview of Unified InverNet Framework in VFL.

$\mathbb{P}_{\text{target}}$. The Data Passive Attack only requires the attacker to own i.i.d. dataset as the target’s private data, while the Isolated Query Attack assumes the attacker can make queries to $\mathbb{P}_{\text{target}}$ but has no auxiliary dataset. In the Stealth Attack scenario, the attacker can neither make queries nor has i.i.d. data but has obtained a minimal amount of the target’s private data used in training its bottom model.

4. UIFV Framework Overview

We have developed a comprehensive framework, the Unified InverNet Framework in VFL (UIFV), which enables attackers with varying capabilities to train an InverNet and use it to reconstruct private data.

In the VFL framework, we consider the bottom model f_k of participant \mathbb{P}_k as a feature extractor. The bottom model f_k generates the intermediate features H^k that are fed into the top model f_{top} . Considering that the intermediate layers of neural networks retain rich semantic information of input data, the proposed UIFV framework focuses on training an InverNet g that establishes the relationship $g(f_k(x^k)) = x^k$, which can then be used to upsample and reconstruct the private data x^k . The objective function for training the InverNet g can be formulated as:

$$\arg \min_{\theta_g} \left\| g(f_k(x^k)) - x^k \right\|^2, \quad (2)$$

which indicates that the private data x^k and the bottom model f_k are required for training the InverNet. However, such information cannot be directly obtained in realistic VFL scenarios. Therefore, Data Preparation and Model Preparation are two key functional modules in the proposed UIFV framework that respectively prepare the model and data information needed for training the InverNet.

The Data Preparation module may be implemented in different ways based on the attacker’s capabilities. If the attacker possesses an i.i.d. auxiliary dataset \tilde{x}^k , it can be leveraged as a substitute for the private data x^k . If the attacker does not own such auxiliary data, the Data Preparation function can be realized through a data generator that utilizes the prior information of the original data (such as data distribution characteristics) to generate synthetic data x^{fake} .

Similarly, different methods can be employed by the Model Preparation module based on the attacker’s capabilities. If the attacker can make inference queries to the target party, which is reasonable in the VFL architecture, then the model output $f_k(x^k)$ can be obtained from the queries. If the attacker cannot make query requests to the bottom model, then the attacker may train a shadow model \tilde{f}_k to replace the model f_k for training the InverNet.

After completing the training of InverNet g in UIFV, the intermediate features H^{target} received from the target party can be passed to the InverNet g to obtain an estimate \hat{x}^{target} of the original private data x^{target} .

As depicted in Figure 2, the UIFV framework encompasses three distinct stages. The Data Preparation and Model Preparation functions are performed in the initial stage to prepare the pertinent data and model needed for training the InverNet, which is then conducted in the second stage. Then, in the final stage, the pretrained InverNet is employed to reconstruct the private data used for model training by the target party.

5. Four Attack Scenarios in UIFV

5.1. Query Attack (QA)

In the Query Attack scenario, the attacker has no access to the target party’s model parameters and model gradient

Algorithm 1: Query Attack

```

1 Function QueryAttack( $f_{\text{target}}, H^{\text{target}}, D^{\text{aux}}$ ):
2    $g_{\text{target}} = \text{TrainInverseNet}(D^{\text{aux}}, f_{\text{target}})$ 
3    $\hat{x}_{\text{target}} = \text{Inverse}(g_{\text{target}}, H^{\text{target}})$ 
4   return  $\hat{x}_{\text{target}}$ 
5 Function TrainInverseNet( $D^{\text{aux}}, f_{\text{target}}$ ):
6   while  $n < N\text{Iters}$  do
7     Randomly sample  $x_1, x_2, \dots, x_k$  from  $D^{\text{aux}}$ 
8     Obtain  $H_i$  by querying  $f_{\text{target}}$  with  $x_i$ 
9      $L(g_{\text{target}}) = \frac{1}{m} \sum_{i=1}^m \left\| g_{\text{target}}(H_i) - x_i \right\|^2$ 
10     $\theta_g^{(n+1)} = \theta_g^{(n)} - \epsilon \frac{\partial L(g_{\text{target}}^{(n)})}{\partial \theta_g^{(n)}}$ 
11     $n+ = 1$ 
12  end
13  return  $g_{\text{target}}^{(N\text{Iters})}$ 
14 Function Inverse( $g_{\text{target}}, H^{\text{target}}$ ):
15   $\hat{x}_{\text{target}} = g_{\text{target}}(H^{\text{target}})$ 
16  return  $\hat{x}_{\text{target}}$ 

```

information during the training process, which is consistent with the black-box attack setting Jiang et al. (2022); Liu et al. (2021). On the other hand, the attacker can freely initiate query requests to the target party and possesses the auxiliary dataset $\tilde{x}^{\text{target}}$, that is, i.i.d. with the target party's private data.

$$g = \arg \min_{\theta_g} \frac{1}{m} \sum_{i=1}^m \left\| g(\tilde{H}_i^{\text{target}}) - \tilde{x}_i^{\text{target}} \right\|^2 \quad (3)$$

In this attack scenario, since the attacker owns an auxiliary data set and is able to query the target model, the UIFV framework requires no work for data and model preparation in the first stage. In the second stage, auxiliary data $\tilde{x}^{\text{target}}$ is used to initiate query requests to the target party to obtain the intermediate features $\tilde{H}^{\text{target}}$ output by the target model f_{target} . Subsequently, the obtained $\tilde{H}^{\text{target}}$ and the corresponding $\tilde{x}^{\text{target}}$ are used to train InverNet g , as shown in 3, where m represents the number of samples in the dataset. Then, in the final stage of UIFV, the trained InverNet g can be used for the reconstruction of the target data x^{target} . The complete attack algorithm in the Query Attack scenario is shown in Algorithm 1.

5.2. Data Passive Attack (DPA)

In the scenario of Data Passive Attack, the attacker's capabilities are limited to only possessing the i.i.d. auxiliary dataset D^{aux} without the ability to query the target party. This could be because the target party only participates in the VFL training process but not the inference stage. In such an attack scenario, Under this assumption, the Model Preparation function in the UIFV framework needs to construct a

Algorithm 2: Data Passive Attack

```

1 Function DataPassiveAttack( $f_{\text{target}}, H^{\text{target}}, D^{\text{aux}}$ ):
2    $\tilde{f}_{\text{target}} = \text{TrainShadowModel}(D^{\text{aux}}, f_{\text{top}})$ 
3    $g_{\text{target}} = \text{TrainInverseNet}(D^{\text{aux}}, \tilde{f}_{\text{target}})$ 
4    $\hat{x}_{\text{target}} = \text{Inverse}(g_{\text{target}}, H^{\text{target}})$ 
5   return  $\hat{x}_{\text{target}}$ 
6 Function TrainShadowModel( $D^{\text{aux}}, f_{\text{target}}$ ):
7   while  $n < N\text{Iters}$  do
8     Randomly sample  $x_1, x_2, \dots, x_k$  and labels
9      $y_1, y_2, \dots, y_k$  from  $D^{\text{aux}}$ 
10     $\hat{y}_i = f_{\text{top}}(H^1, \dots, \tilde{f}_{\text{target}}(x_i), \dots, H^K)$ 
11     $L(\tilde{f}_{\text{target}}) = \frac{1}{k} \sum_{i=1}^k y_i \hat{y}_i + (1 - y_i)(1 - \hat{y}_i)$ 
12     $\theta_{\tilde{f}}^{(n+1)} = \theta_{\tilde{f}}^{(n)} - \epsilon \frac{\partial L(\tilde{f}_{\text{target}}^{(n)})}{\partial \theta_{\tilde{f}}^{(n)}}$ 
13     $n+ = 1$ 
14  end
15  return  $\tilde{f}_{\text{target}}^{(N\text{Iters})}$ 

```

shadow model $\tilde{f}_{\text{target}}$ that mimics the behavior of the target model.

One approach to building a shadow model is to recover the structure and parameters of the target model by querying the black-box model, allowing the shadow model to mimic the behavior of the target model Oh et al. (2019); Tramèr et al. (2016); Wang and Gong (2018). However, since we cannot query the target model, we turn to the VFL architecture and attempt to build a model that behaves similarly to the target model within the VFL framework. In this process, we require the cooperation of other participants, querying them with i.i.d. data to obtain the corresponding intermediate features. The optimization objective of the shadow model is

$$\arg \min_{\tilde{f}} \frac{1}{m} \sum_{i=1}^m \mathcal{L}(f_{\text{top}}(H^1, \dots, \tilde{f}_{\text{target}}(x_i), \dots, H^K), y_i), \quad (4)$$

where m represents the number of samples in the dataset, and H^k is the intermediate features output of other participants, which remains constant during the training process. \mathcal{L} is consistent with the loss function of the top model. This means that the training of $\tilde{f}_{\text{target}}$ is guided by the supervision of f_{top} .

Once the shadow model $\tilde{f}_{\text{target}}$ is trained in the first stage, it can be used in the role of f_{target} together with the dataset D^{aux} to train the InverNet g in the second stage and then to reconstruct the private data in the third stage of the UIFV framework, as in the Query Attack scenario. The complete attack algorithm in the Data Passive Attack scenario is shown in Algorithm 2.

Algorithm 3: Isolated Query Attack

```

1 Function IsolatedQueryAttack( $f_{target}, H^{target}, T$ ):
2    $D^{fake} = \text{DataGeneration}(T)$ 
3    $g_{target} = \text{TrainInverseNet}(D^{fake}, f_{target})$ 
4    $\hat{x}_{target} = \text{Inverse}(g_{target}, H^{target})$ 
5   return  $\hat{x}_{target}$ 
    
```

5.3. Isolated Query Attack (IQA)

In the Isolated Query Attack scenario, we assume that the attacker can freely initiate queries to the target party but does not have the i.i.d. data. Facing this situation, in the first stage of the UIFV framework, the Data Preparation module implements a Data Generator to create a set of fake data that are then used for querying the target part to obtain the intermediate features.

The most straightforward approach to creating fake data is random generation; for example, sampling pure noise from a standard Gaussian distribution as in He et al. (2019) for image data. However, tabular data, which is significantly different in distribution from image data, consists of heterogeneous features and lacks spatial or semantic relationships, making it more complex to discover and utilize relationships Borisov et al. (2022). Therefore, using randomly generated data for query requests may lead to poor reconstruction results, as verified in Section 6.4.2.

To address this issue, we introduce prior knowledge to guide the process of generating random data, aiming to enhance the quality of data reconstruction. For image data, we focus on generating smoother random samples by reducing the influence of noise and outliers in random data through sampling from a standard Gaussian distribution. For tabular data, based on the analysis in Borisov et al. (2022), we utilize the header information of the target dataset to construct pseudo data, making the fabricated data closer to the distribution of real data. For categorical variables, we adopt a one-hot encoding approach, randomly selecting a category to set its corresponding column to 1, while keeping other columns at 0. For continuous variables, we first estimate the range of values based on experience and then perform random sampling within the estimated range using a uniform distribution. We call this process the data generation module.

The generated fake data D^{fake} will be used in the second stage to train InverNet g . Then, in the final stage of the UIFV framework, the trained InverNet g will be used to reconstruct private data. The complete attack algorithm in the Isolated Query Attack scenario is shown in Algorithm 3.

5.4. Stealth Attack (SA)

In the previous three attack scenarios, the attacker can possess an i.i.d. auxiliary dataset and/or make queries to obtain the intermediate features but does not know about the target party's private information. In this scenario, even if the attacker loses both the auxiliary data and the query capabilities, data reconstruction is still possible if the attacker \mathbb{P}_{adv} may acquire a minimal amount of the target party's private

Algorithm 4: Stealth Attack

```

1 Function StealthAttack( $H^{target}, D^{priv}$ ):
2    $g_{target} = \text{TrainInverseNet2}(H^{target}, D^{priv})$ 
3    $\hat{x}_{target} = \text{Inverse}(g_{target}, H^{target})$ 
4   return  $\hat{x}_{target}$ 

5 Function TrainInverseNet2( $H^{target}, D^{priv}$ ):
6    $g_{target}^{(0)} = \text{Init}()$ 
7   while  $n < N\text{Iters}$  do
8     Obtain leaked samples  $x_1, x_2, \dots, x_k$  from
        $D^{priv}$ 
9     Prepare  $H_i$  data corresponding to  $x_i$ 
10     $L(g_{target}) = \frac{1}{m} \sum_{i=1}^m \left\| g_{target}(H_i) - x_i \right\|^2$ 
11     $\theta_g^{(n+1)} = \theta_g^{(n)} - \epsilon \frac{\partial L(g_{target}^{(n)})}{\partial \theta_g^{(n)}}$ 
12     $n++ = 1$ 
13  end
14  return  $g_{target}^{(N\text{Iters})}$ 
    
```

data and explicitly knows that these data have already been used in the VFL process. For instance, \mathbb{P}_{adv} might collude with some internal employees of the target party (whose data are jointly maintained by both parties) to secretly acquire a small subset of data, which is considered possible as has been noted in some studies on analogous VFL scenarios, such as Zeng et al. (2023). The knowledge of some private data used by the target party allows the attacker to start from the second stage of the UIFV framework to directly train InverNet g with the objective function simplified to 5:

$$\arg \min_{\theta_g} \left\| g(H^k) - x^k \right\|^2 \quad (5)$$

In this equation, x^k signifies the secretly acquired data, while H^k represents the corresponding intermediate features of these secret data. Then, the trained g will be used in the third stage to complete private data reconstruction. The complete attack algorithm in the Stealth Attack scenario is shown in Algorithm 4.

6. Experiments

6.1. Experiment Setting

In the following content, we will describe our experimental design, focusing on two parts: the datasets used and the models implemented.

6.1.1. Datasets

In our experiments, we employed four public datasets: Bank marketing analysis Moro et al. (2014)¹ (Bank), Adult income Becker and Kohavi (1996)² (Adult), Default of credit

¹<https://archive.ics.uci.edu/dataset/222/bank+marketing>

²<https://archive.ics.uci.edu/dataset/2/adult>

Dataset	Bank	Adult	Credit	CIFAR10
Sample Num.	41,188	32,561	30,000	60,000
Feature Num.	20	14	23	$32 \times 32 \times 3$
Class Num.	2	2	2	10
Accuracy on VFL	0.9153	0.8417	0.8322	0.7493
AUC on VFL	0.8254	0.8969	0.7844	-

Table 2

Dataset used in our experiments.

card clients Yeh and Lien (2009)³ (Credit) and CIFAR10 Krizhevsky et al. (2009)⁴, to evaluate our methods. These datasets range from banking marketing analysis to image recognition, each with its unique features and challenges. For data preparation, continuous columns in tabular datasets were scaled, and discrete columns were one-hot encoded. We have summarized the evaluated datasets in Table 2.

The Bank dataset, derived from a Portuguese banking institution’s direct marketing campaigns, encompasses 41188 samples with 20 features and two classes to determine the likelihood of clients subscribing to a term deposit, featuring inputs like age, job, marital status, and education. The Adult dataset, also known as the "Census Income" dataset, includes 32561 instances with 14 features such as age, workclass, and education, and it aims to predict if an individual’s income surpasses \$50,000 per annum using census data. The Credit dataset, sourced from Taiwan, comprises 30,000 instances with 23 features, including credit amount, gender, education, and marital status, and aims to predict the probability of default payments in credit card clients using various data mining methods. The CIFAR10 dataset is a widely-used public dataset for computer vision research, containing 60,000 color images with a resolution of 32×32 pixels, divided into ten categories with 6,000 images in each category. Additionally, before training the models, we scaled the continuous columns in the tabular datasets to the range of $[-1, 1]$, while the discrete columns were encoded using one-hot encoding.

6.1.2. Models

For simplicity, we chose to focus on a two-party VFL setup in our experiment. Theoretically, this framework can be expanded to scenarios with any number of participants. In our attack scenario, VFL involves two roles: one is the active party, which plays the role of the adversary and possesses a complete top model and a bottom model; the other is the passive participant, serving as the target of the attack, equipped only with a bottom model. Regarding data splitting, unless specifically stated otherwise, it is generally assumed that the active and passive parties equally share the data. For tabular data, discrete and continuous data each constitute half; for image data, each image is bisected along the central line, with both parties holding half, but only the active party possesses the data labels. In terms of model construction, for

processing tabular data, both parties use a three-layer fully connected neural network as the bottom model. The top-layer model is also composed of a three-layer fully connected network, with each layer incorporating a ReLU activation function. For models processing image data, both parties employ a network comprising two convolutional layers and one pooling layer as the bottom model, while the top model consists of four convolutional layers and two fully connected layers, with each layer also integrating a ReLU activation function. Upon applying this VFL architecture to four different datasets, we achieved the training performance results as shown in Table 2.

The InverNet for all bottom models is consistent with the architecture of the respective bottom model. For tabular data, the inverse net utilizes a three-layer fully connected neural network, while for image data, the model employs two transposed convolutional layers and one pooling layer.

To ascertain the effectiveness of our proposed method, on the tabular data set, we conducted comparative evaluations against two types of Vertical Federated Learning (VFL) data reconstruction attacks. Firstly, we compared our approach to a Generative Model Reconstruction Attack under a white-box scenario, denoted as GRN Luo et al. (2021). Secondly, we assessed against a black-box scenario where a shadow model is trained prior to launching a white-box attack, referred to as GIA Jiang et al. (2022). Lastly, we included a random guessing baseline method to benchmark the inherent performance of random speculation. On the image dataset, we compared our method with split learning data reconstruction attack approaches He et al. (2019), namely Black-box attack and Query-free attack methods.

In pursuit of a fair comparison with other methodologies, our model’s architecture mirrors that of GRN Luo et al. (2021) in terms of the number of parameters, featuring three hidden layers with neuron counts of 600, 300, and 100. We designed our individual bottom models with 300, 100, and 100 neurons in their hidden layers. We also took care to ensure that the GIA method Jiang et al. (2022) we implemented utilized an equivalent number of model parameters for an accurate comparison. Moreover, despite the original GIA method not incorporating nonlinear activation functions, we introduced them into the target party’s model to ensure the fairness of the comparison. For the reconstruction method of image data, we use the same model architecture. However, unlike the split learning model, the VFL has two separate bottom models that are trained independently.

6.2. Evaluation Metrics

In our work, we evaluated two categories of data: tabular and image data, employing distinct metrics for each category.

For image data, we adopt two widely recognized metrics: Peak Signal-to-Noise Ratio (PSNR) and Structural Similarity Index (SSIM) Wang et al. (2004). PSNR quantifies image errors by calculating the mean squared error between origin and attack images, with higher values indicating lower quality degradation. SSIM evaluates image quality based

³<https://archive.ics.uci.edu/dataset/350/default+of+credit+card+clients>

⁴<https://www.cs.toronto.edu/~kriz/cifar.html>

Dataset	Evaluation	UIFV-QA	UIFV-DPA	UIFV-IQA	UIFV-SA	GRN	GIA	Random
Bank	Accuracy	98.0 ± 0.1	95.7 ± 0.4	66.2 ± 1.4	90.1 ± 0.1	30.2 ± 6.7	55.9 ± 1.8	21.0 ± 0.0
	Discrete Acc	99.5 ± 0.0	99.0 ± 0.1	87.8 ± 2.1	94.9 ± 0.3	29.4 ± 8.0	82.6 ± 4.5	26.9 ± 0.1
	Continuous Acc	96.4 ± 0.2	92.4 ± 0.8	44.6 ± 1.2	85.2 ± 0.3	30.5 ± 10.5	29.3 ± 3.3	15.1 ± 0.1
Adult	Accuracy	98.5 ± 0.0	80.8 ± 0.9	94.8 ± 0.5	72.8 ± 3.4	41.1 ± 8.5	18.9 ± 8.3	11.1 ± 0.1
	Discrete Acc	98.4 ± 0.0	81.1 ± 0.9	98.1 ± 0.6	71.4 ± 2.4	41.9 ± 6.4	23.4 ± 10.1	9.0 ± 0.1
	Continuous Acc	98.8 ± 0.1	79.8 ± 1.2	81.7 ± 0.7	78.3 ± 8.6	37.3 ± 22.9	0.9 ± 1.0	19.8 ± 0.1
Credit	Accuracy	98.2 ± 0.1	96.0 ± 0.5	44.3 ± 1.6	93.8 ± 0.2	53.8 ± 25.8	41.1 ± 2.8	13.9 ± 0.1
	Discrete Acc	98.5 ± 0.1	97.1 ± 0.5	75.2 ± 4.8	92.2 ± 0.3	76.7 ± 25.9	88.4 ± 5.7	10.6 ± 0.1
	Continuous Acc	98.0 ± 0.2	95.3 ± 0.6	26.6 ± 1.8	94.8 ± 0.2	51.9 ± 26.6	14.0 ± 3.4	15.7 ± 0.1

Table 3

Performance comparison with state-of-the-art methods on the bank, adult, and credit datasets. (Best results are highlighted in bold.)

	QA	DPA	IQA	SA	Black-box	Query-free
PSNR	23.83	25.61	14.92	22.32	19.81	12.74
SSIM	0.85	0.89	0.58	0.81	0.69	0.18

Table 4

Performance comparison with data reconstruction methods used in split learning on the CIFAR10 dataset. Here, QA, DPA, IQA, and SA represent the results of UIFV in four different scenarios, while Black-box and Query-free are from comparative methods. (Best results are highlighted in bold.)

on structural information, brightness, and contrast, ranging from 0 to 1, with 1 indicating perfect similarity.

In evaluating tabular data, previous studies Luo et al. (2022, 2021) have used training loss or distance measures to assess reconstruction accuracy. However, these methods may not align with real attack scenarios, which focus on whether reconstructed categories match the actual ones. To address these issues, we adopted the metrics proposed in Vero et al. (2022). Considering the characteristics of tabular data, we separate the treatment of categorical and continuous features. For vector x and its reconstruction vector \hat{x} , the accuracy metric is defined as follows:

$$\text{accuracy}(x, \hat{x}) := \frac{1}{M + L} \left(\sum_{i=1}^M \mathbb{I}\{x_i^D = \hat{x}_i^D\} + \sum_{i=1}^L \mathbb{I}\{\hat{x}_i^C \in [x_i^C - \varepsilon, x_i^C + \varepsilon]\} \right), \quad (6)$$

where M and L denote the number of discrete variables and continuous variables in vector x . The indicator function \mathbb{I} checks for equality in categorical features and for the continuous features being within an epsilon range ε .

6.3. Performance Evaluation and Comparison

In our VFL data reconstruction attack experiments, we conducted a comprehensive comparison between our proposed UIFV method and state-of-the-art approaches on bank, adult, and credit datasets. Additionally, we compared

UIFV against split learning methods on CIFAR-10. We conducted experiments using the UIFV method in four different scenarios, while for the comparison methods, we tested them only in their respective originally proposed specific scenarios. We utilized the evaluation metrics from Section 6.2 and set the epsilon value for continuous features to 0.2. Detailed results can be found in Tables 3 and 4.

The research findings indicate that our UIFV method significantly outperformed the comparison methods in terms of reconstruction accuracy across the four different scenarios. The QA scenario, with its relaxed scenario assumptions, excelled across datasets, surpassing 96% in overall, discrete, and continuous accuracy on bank and adult datasets. Its continuous accuracy reached $96.4\% \pm 0.2$ on the bank dataset and $98.8\% \pm 0.1$ on the adult dataset, outperforming other methods like GRN and GIA, which had much lower rates. Similarly, DPA, IQA, and SA scenarios showed robust performance, with most outcomes exceeding 60% accuracy. Compared to GRN and GIA, our methods demonstrated superior performance across all metrics. For instance, IQA and SA showed lower accuracies of $66.2\% \pm 1.4$ and $90.1\% \pm 0.1$ on the bank dataset, while GRN and GIA lagged further behind.

In the experimental section of Section 6, we conducted detailed reconstruction experiments on the image dataset, using two metrics, PSNR and SSIM, to measure the effectiveness of the reconstruction. However, while these metrics can assess our results from a technical standpoint, they are not sufficient to intuitively display the actual effects of the attack. Therefore, Figure 3 directly presents some specific reconstruction results, vividly demonstrating the actual effectiveness of our attack method.

We conducted reconstruction experiments on the CIFAR10 image dataset using two metrics, PSNR and SSIM, to measure the effectiveness of our UIFV method. In the DPA scenario, we achieved the highest scores with a PSNR of 25.61 and an SSIM of 0.89, demonstrating robustness in maintaining image quality. These values significantly surpassed those of comparative methods; the Black-box approach scored a PSNR of 19.81 and an SSIM of 0.69, while the Query-free method registered markedly lower

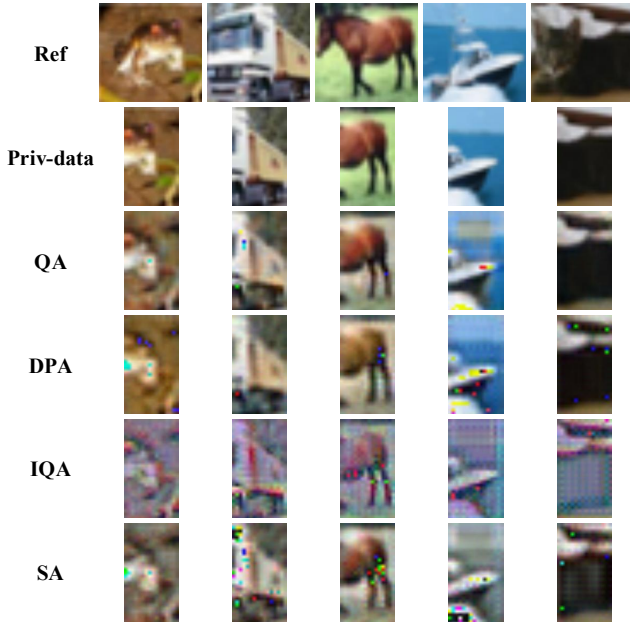


Figure 3: Our method is applied to the CIFAR10 dataset. The first line is the original image, the second and second lines are the private data that needs to be reconstructed during the VFL process, and the last four lines are the reconstruction effects under the four scenes.

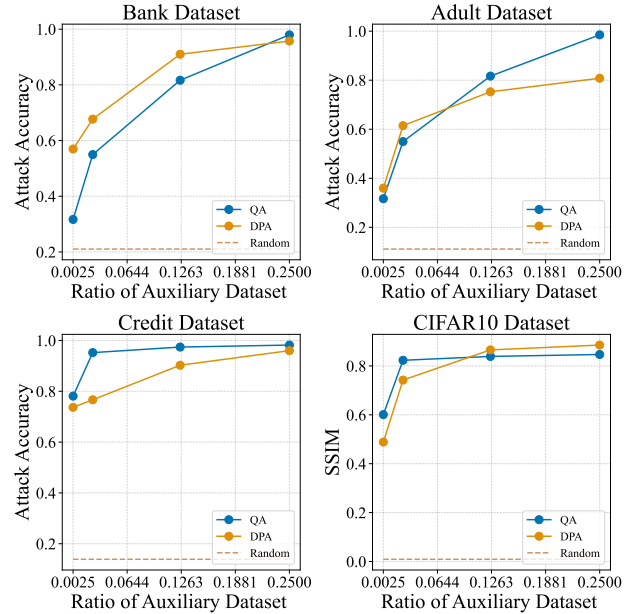


Figure 5: The size ratio of the auxiliary dataset relative to the training dataset.

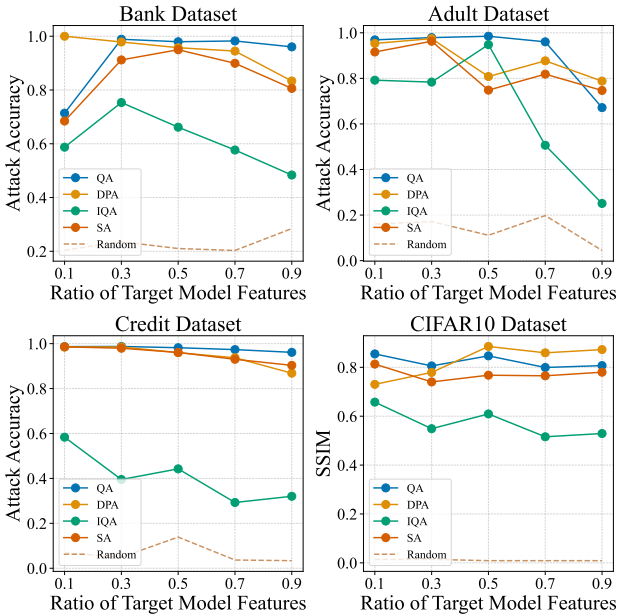


Figure 4: The attack accuracy of the target model with different ratios of features.

scores of 12.74 and 0.18, respectively. Our UIFV method also showed commendable performance in other scenarios. To visually illustrate our attack outcomes, we present some actual reconstruction results in Figure 3.

6.3.1. Attack Effectiveness at Different Feature Splitting Ratios

To explore realistic VFL scenarios with multiple parties holding different feature proportions, we tested various scenarios where the target party’s feature proportion varied. We simulated five scenarios with two participants, where the target party’s feature proportions were 0.1, 0.3, 0.5, 0.7, and 0.9, representing a range from highly imbalanced to balanced feature splitting. We evaluated our methods across four datasets, comparing them with random guessing.

The results, depicted in Figure 4, show that different methods performed variably across feature splitting ratios and datasets. Generally, QA, DPA, and SA methods yielded stable and effective results, with attack accuracy rates over 60%, indicating significant privacy risks. The IQA method was less stable but still outperformed random guessing.

6.4. Ablation Study

6.4.1. Size of the auxiliary dataset

Among the four attack scenarios, QA and DPA rely on i.i.d. auxiliary datasets for data reconstruction. Our study found a direct correlation between the auxiliary dataset size and reconstruction accuracy.

We tested four sizes of auxiliary datasets: 0.0025, 0.025, 0.125, and 0.25, representing their relative sizes to the VFL training dataset. Results in Figure 5 show that as the auxiliary dataset size increases, the reconstruction accuracy of our method improves. This suggests that a larger auxiliary dataset, offering more information, allows for a more accurate estimation of the original dataset’s distribution, thus enhancing reconstruction accuracy.

Dataset	Evaluation	IQA-No-DG	IQA
Bank	Accuracy	27.19 ± 5.27	66.17 ± 1.43
	Discrete Acc	42.30 ± 9.59	87.78 ± 2.11
	Continuous Acc	12.08 ± 1.19	44.57 ± 1.21
Adult	Accuracy	53.09 ± 3.59	94.81 ± 0.54
	Discrete Acc	57.88 ± 4.64	98.08 ± 0.57
	Continuous Acc	33.95 ± 2.42	81.72 ± 0.71
Credit	Accuracy	14.35 ± 2.56	44.25 ± 1.61
	Discrete Acc	36.94 ± 7.06	75.17 ± 4.78
CIFAR10	Continuous Acc	1.45 ± 0.26	26.59 ± 1.84
	PSNR	14.26 ± 0.16	14.93 ± 0.49
	SSIM	0.56 ± 0.01	0.58 ± 0.04

Table 5

Comparative Performance of IQA with and without Data Generation Module Across Different Datasets. (Best results are highlighted in bold.)

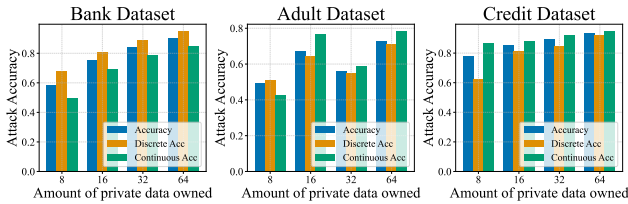


Figure 6: The relationship between the amount of private data owned and attack accuracy on the bank, adult and credit datasets.

6.4.2. Impact of Data Generation

In the IQA attack scenario, we utilize a Data Generator (DG) to enhance the accuracy of reconstruction attacks. To assess the DG module’s effectiveness, we compared it with a random number generator simulating a uniform distribution. Results in Table 5 show that IQA with the DG module significantly improved performance on all tabular datasets and metrics, averaging a 30% increase in accuracy, with notable gains in image datasets. This demonstrates the DG module’s vital role in simulating the original dataset’s distribution and increasing attack accuracy, in contrast to the lower performance with a simple random number generator. Hence, the DG module is essential for successful data reconstruction attacks.

6.4.3. Size of the Known Private Dataset

In the SA attack scenario, we assume that the attacker has acquired a small number of the target’s private data to train an InverNet for data reconstruction. We evaluated the attack’s efficacy with varying numbers of prior-known private samples, 8, 16, 32, and 64, as shown in Figure 6 and Table 6.

The results indicate a positive correlation between the number of training samples and the accuracy metrics (general, categorical, continuous, PSNR, and SSIM). This demonstrates that even with a minimal amount of training data, such as 8 samples, our method can still be successful and yield reasonable results.

x^{priv} num.	8	16	32	64
PSNR	19.31	21.00	21.59	22.32
SSIM	0.74	0.78	0.79	0.81

Table 6

The relationship between the amount of private data owned on the CIFAR10 dataset and the reconstruction effect.

6.4.4. The Impact of InverNet Model Size on Attack Effectiveness

As a crucial component of the UIFV framework, we delved into the impact of the size of the InverNet model on our attack performance. For attacks on tabular data, we employed InverNet, which is composed of three fully connected layers. During the experiments, we assessed the specific effects of one and two fully connected layers on the effectiveness of the attack. Similarly, for attacks on image data, we used InverNet constructed with two layers of transposed convolution, and evaluated the impact of one and three layers of transposed convolution on the results of the attack.

The experimental results are shown in Table 7. The results showed that as the number of layers and the size of the InverNet model increased, there was a certain degree of enhancement in the performance of UIFV attacks. However, overall, while increasing the number of layers in InverNet does improve performance, once it exceeds a certain threshold, the growth in performance tends to saturate. When applying the UIFV framework, choosing the appropriate size of the InverNet model is particularly important, necessitating careful adjustment and selection based on different data types and attack scenarios.

6.5. Defense evaluation

Although this study primarily focuses on attack strategies, we have also examined several defensive measures. Particularly, effective defense methods such as Differential Privacy (DP), noise addition, purification defense strategies Yang et al. (2023), and the adaptive obfuscation privacy protection strategy FedPass Gu et al. (2023) have been considered. Differential privacy technology demonstrates significant potential in defending against data reconstruction attacks by adding noise to gradients during the training process, thereby protecting individual data privacy while maintaining the overall effectiveness of the model. The method of adding noise to model outputs hinders attackers from obtaining precise information, thus protecting the data from malicious use, although this may impact the accuracy of the model. Purification defense strategies use technologies like Autoencoders to reduce the variability in model outputs, enhance privacy protection, and decrease the distinguishability between outputs, thereby reducing the likelihood of attackers using model outputs for inference. FedPass, as a novel defense framework, is particularly suitable for Vertical Federated Learning (VFL) environments, employing adaptive obfuscation techniques to protect data privacy while allowing contributions from various parties.

Bank					Adult				
Layers	QA	DPA	IQA	SA	Layers	QA	DPA	IQA	SA
1	95.39	93.51	58.09	89.12	1	92.45	86.67	76.08	86.50
2	97.66	95.95	59.85	89.30	2	93.33	86.23	75.10	86.44
3	97.96	95.74	66.17	90.07	3	98.49	80.80	94.81	72.79

Credit					CIFAR10				
Layers	QA	DPA	IQA	SA	Layers	QA	DPA	IQA	SA
1	97.73	94.01	40.40	90.30	1	0.70	0.76	0.54	0.70
2	98.15	95.93	40.89	93.56	2	0.85	0.89	0.61	0.81
3	98.19	95.99	44.25	93.83	3	0.86	0.90	0.62	0.83

Table 7

The Impact of InverNet Model Size on Attack Effectiveness. For each dataset, the first column represents the number of layers of InverNet, and the last four columns indicate the effectiveness of our attack method under four different scenarios. For CIFAR10, SSIM is the Evaluation Metric for the Last Four Columns.

Bank						Adult					
Ratio	AUC	QA	DPA	IQA	SA	Ratio	AUC	QA	DPA	IQA	SA
1	85.89	86.38	88.29	18.96	18.96	1	88.79	87.78	84.92	73.92	73.87
0.5	93.80	97.46	95.40	52.80	18.96	0.5	87.71	92.27	87.59	84.15	83.07
0.1	93.84	97.93	95.50	64.01	78.16	0.1	87.62	93.51	89.29	82.91	81.45
0.01	93.81	98.31	96.02	69.68	89.48	0.01	86.95	95.44	88.56	82.94	87.50
0.001	93.92	98.22	96.04	66.40	90.49	0.001	86.66	95.86	89.15	61.72	85.48

Credit						CIFAR10					
Ratio	AUC	QA	DPA	IQA	SA	Ratio	ACC	QA	DPA	IQA	SA
1	77.03	96.75	92.87	28.92	88.46	1	61.99	0.70	0.85	0.34	0.11
0.5	76.02	96.52	96.52	26.04	90.45	0.5	67.26	0.14	0.81	0.14	0.0
0.1	77.36	97.95	96.00	39.92	93.13	0.1	72.99	0.72	0.87	0.44	0.68
0.01	77.16	97.59	96.25	41.50	93.26	0.01	74.84	0.80	0.88	0.53	0.74
0.001	76.48	98.36	95.09	41.05	93.29	0.001	74.25	0.86	0.89	0.57	0.81

Table 8

Experimental Results of DP Defense. For each dataset, the first column represents the ratio of the defense, the second column shows the results of the VFL task, and the last four columns indicate the effectiveness of our attack method under four different scenarios. For CIFAR10, SSIM is the Evaluation Metric for the Last Four Columns.

To assess the robustness of our UIFV method, we implemented two representative data reconstruction defense methods within the VFL framework, namely Differential Privacy and Gaussian noise addition, to test the performance of UIFV. In our experiments, we set the noise ratio to 1, 0.5, 0.1, 0.01, and 0.001, respectively, and conducted experiments across four different scenarios in four datasets. The experimental results of Differential Privacy are shown in Table 8, and those of noise addition are in Table 9.

Overall, these two defense methods do indeed have an effect in reducing the efficacy of data reconstruction attacks. However, the impact of these methods on the effectiveness of attacks is relatively limited. In scenarios such as QA, DPA, and IQA, a certain success rate of attacks can still be maintained even with a high noise ratio. In the SA scenario, the impact of these two defense methods is more noticeable. As the noise ratio increases, there is a downward trend in the attack accuracy in the SA scenario.

7. Conclusion

In our paper, we introduce the Unified InverNet Framework in VFL (UIFV) a novel approach for conducting data reconstruction attacks in VFL environments. This method diverges from traditional attack strategies by utilizing the intermediate features of the target model instead of relying on gradient information or model information. UIFV demonstrates exceptional adaptability, suitable for various black-box scenarios. Experiments conducted on four benchmark datasets show that our approach surpasses the existing attack methods in effectiveness, achieving over 96% accuracy in scenarios like QA. Through in-depth ablation studies, we also confirm the significance of key components such as the data generation module. This research highlights the significant privacy risks faced by VFL systems and underscores the urgent need to establish robust defense mechanisms to counter such attacks.

Bank						Adult					
Ratio	AUC	QA	DPA	IQA	SA	Ratio	AUC	QA	DPA	IQA	SA
1	93.68	18.96	89.19	49.02	18.96	1	88.53	70.87	69.93	56.21	3.07
0.5	93.94	98.52	94.51	64.81	18.96	0.5	89.18	91.20	71.88	90.92	3.07
0.1	94.01	98.22	95.48	67.16	90.67	0.1	87.02	96.37	90.68	73.40	87.19
0.01	93.95	97.85	95.59	63.60	88.81	0.01	88.55	91.14	82.20	72.69	83.50
0.001	93.85	98.26	96.20	60.42	91.19	0.001	86.81	94.90	89.17	78.52	86.16
Credit						CIFAR10					
Ratio	AUC	QA	DPA	IQA	SA	Ratio	ACC	QA	DPA	IQA	SA
1	76.90	98.13	87.77	62.98	3.46	1	64.97	0.75	0.79	0.59	0.0
0.5	77.51	98.35	96.08	57.51	94.34	0.5	66.81	0.88	0.79	0.62	0.07
0.1	76.92	98.04	96.20	33.98	91.86	0.1	74.41	0.86	0.83	0.59	0.82
0.01	77.23	97.89	96.24	37.66	91.96	0.01	74.13	0.81	0.87	0.56	0.76
0.001	76.81	97.54	95.35	33.91	92.52	0.001	74.38	0.80	0.90	0.57	0.90

Table 9

Experimental Results of Gaussian noise Defense. For each dataset, the first column represents the ratio of the defense, the second column shows the results of the VFL task, and the last four columns indicate the effectiveness of our attack method under four different scenarios. For CIFAR10, SSIM is the Evaluation Metric for the Last Four Columns.

8. CRediT authorship contribution statement

Jirui Yang: Methodology, Writing - original draft. **Peng Chen:** Methodology, Writing - review and editing. **Zhihui Lu:** Methodology, Supervision, Writing- review and editing. **Qiang Duan:** Methodology, Writing - review and editing. **Yubing Bao:** Formal analysis, Data curation.

9. Declaration of Competing Interest

The authors declare that they have no known competing financial interests or personal relationships that could have appeared to influence the work reported in this paper.

10. Acknowledgements

The work of this paper is supported by the National Key Research and Development Program of China (2022YFC3302300, 2021YFC3300600), National Natural Science Foundation of China under Grant (No. 92046024, 92146002, 61873309), and Shanghai Science and Technology Innovation Action Plan Project under Grant (No.22510761000).

References

- Becker, B., Kohavi, R., 1996. Adult. UCI Machine Learning Repository. DOI: <https://doi.org/10.24432/C5XW20>.
- Borisov, V., Leemann, T., Seßler, K., Haug, J., Pawelczyk, M., Kasneci, G., 2022. Deep neural networks and tabular data: A survey. *IEEE Transactions on Neural Networks and Learning Systems*.
- Chen, J., Huang, G., Zheng, H., Yu, S., Jiang, W., Cui, C., 2022. Graph-fraudster: Adversarial attacks on graph neural network-based vertical federated learning. *IEEE Transactions on Computational Social Systems* 10, 492–506.
- Chen, T., Jin, X., Sun, Y., Yin, W., 2020. Vaff: a method of vertical asynchronous federated learning. *arXiv preprint arXiv:2007.06081*.
- Geiping, J., Bauermeister, H., Dröge, H., Moeller, M., 2020. Inverting gradients-how easy is it to break privacy in federated learning? *Advances in Neural Information Processing Systems* 33, 16937–16947.
- Gu, H., Luo, J., Kang, Y., Fan, L., Yang, Q., 2023. Fedpass: Privacy-preserving vertical federated deep learning with adaptive obfuscation. *arXiv preprint arXiv:2301.12623*.
- He, Z., Zhang, T., Lee, R.B., 2019. Model inversion attacks against collaborative inference, in: *Proceedings of the 35th Annual Computer Security Applications Conference*, pp. 148–162.
- He, Z., Zhang, T., Lee, R.B., 2020. Attacking and protecting data privacy in edge–cloud collaborative inference systems. *IEEE Internet of Things Journal* 8, 9706–9716.
- Jiang, X., Zhou, X., Grossklags, J., 2022. Comprehensive analysis of privacy leakage in vertical federated learning during prediction. *Proc. Priv. Enhancing Technol.* 2022, 263–281.
- Jin, X., Chen, P.Y., Hsu, C.Y., Yu, C.M., Chen, T., 2021. Cafe: Catastrophic data leakage in vertical federated learning. *Advances in Neural Information Processing Systems* 34, 994–1006.
- Kang, Y., Luo, J., He, Y., Zhang, X., Fan, L., Yang, Q., 2022. A framework for evaluating privacy-utility trade-off in vertical federated learning. *arXiv preprint arXiv:2209.03885*.
- Khan, A., ten Thij, M., Wilbik, A., 2022. Communication-efficient vertical federated learning. *Algorithms* 15, 273.
- Krizhevsky, A., Hinton, G., et al., 2009. Learning multiple layers of features from tiny images.
- Li, A., Zhang, L., Tan, J., Qin, Y., Wang, J., Li, X.Y., 2021a. Sample-level data selection for federated learning, in: *IEEE INFOCOM 2021-IEEE Conference on Computer Communications*, IEEE. pp. 1–10.
- Li, A., Zhang, L., Wang, J., Tan, J., Han, F., Qin, Y., Freris, N.M., Li, X.Y., 2021b. Efficient federated-learning model debugging, in: *2021 IEEE 37th International Conference on Data Engineering (ICDE)*, IEEE. pp. 372–383.
- Li, O., Sun, J., Yang, X., Gao, W., Zhang, H., Xie, J., Smith, V., Wang, C., 2022. Label leakage and protection in two-party split learning, in: *International Conference on Learning Representations*. URL: <https://openreview.net/forum?id=cOtBRgsf2fO>.
- Li, W., Milletari, F., Xu, D., Rieke, N., Hancox, J., Zhu, W., Baust, M., Cheng, Y., Ourselin, S., Cardoso, M.J., et al., 2019. Privacy-preserving federated brain tumour segmentation, in: *Machine Learning in Medical Imaging: 10th International Workshop, MLMI 2019, Held in Conjunction with MICCAI 2019, Shenzhen, China, October 13, 2019, Proceedings 10*, Springer. pp. 133–141.
- Liu, Y., Zou, T., Kang, Y., Liu, W., He, Y., Yi, Z., Yang, Q., 2021. Batch label inference and replacement attacks in black-boxed vertical federated learning. *arXiv preprint arXiv:2112.05409*.
- Lu, S., Zhang, Y., Wang, Y., 2020. Decentralized federated learning for electronic health records, in: *2020 54th Annual Conference on*

- Information Sciences and Systems (CISS), IEEE. pp. 1–5.
- Luo, X., Jiang, Y., Xiao, X., 2022. Feature inference attack on shapley values, in: Proceedings of the 2022 ACM SIGSAC Conference on Computer and Communications Security, pp. 2233–2247.
- Luo, X., Wu, Y., Xiao, X., Ooi, B.C., 2021. Feature inference attack on model predictions in vertical federated learning, in: 2021 IEEE 37th International Conference on Data Engineering (ICDE), IEEE. pp. 181–192.
- Moro, S., Cortez, P., Rita, P., 2014. A data-driven approach to predict the success of bank telemarketing. *Decision Support Systems* 62, 22–31.
- Oh, S.J., Schiele, B., Fritz, M., 2019. Towards reverse-engineering black-box neural networks. *Explainable AI: Interpreting, Explaining and Visualizing Deep Learning*, 121–144.
- Pan, X., Zhang, M., Yan, Y., Zhu, J., Yang, Z., 2022. Exploring the security boundary of data reconstruction via neuron exclusivity analysis, in: 31st USENIX Security Symposium (USENIX Security 22), pp. 3989–4006.
- Pasquini, D., Ateniese, G., Bernaschi, M., 2021. Unleashing the tiger: Inference attacks on split learning, in: Proceedings of the 2021 ACM SIGSAC Conference on Computer and Communications Security, pp. 2113–2129.
- Tan, J., Zhang, L., Liu, Y., Li, A., Wu, Y., 2022. Residue-based label protection mechanisms in vertical logistic regression, in: 2022 8th International Conference on Big Data Computing and Communications (BigCom), IEEE. pp. 356–364.
- Tramèr, F., Zhang, F., Juels, A., Reiter, M.K., Ristenpart, T., 2016. Stealing machine learning models via prediction {APIs}, in: 25th USENIX security symposium (USENIX Security 16), pp. 601–618.
- Vero, M., Balunović, M., Dimitrov, D.I., Vechev, M., 2022. Data leakage in tabular federated learning. *arXiv preprint arXiv:2210.01785*.
- Wang, B., Gong, N.Z., 2018. Stealing hyperparameters in machine learning, in: 2018 IEEE symposium on security and privacy (SP), IEEE. pp. 36–52.
- Wang, Z., Bovik, A.C., Sheikh, H.R., Simoncelli, E.P., 2004. Image quality assessment: from error visibility to structural similarity. *IEEE transactions on image processing* 13, 600–612.
- Wei, P., Dou, H., Liu, S., Tang, R., Liu, L., Wang, L., Zheng, B., 2023. Fedads: A benchmark for privacy-preserving cvr estimation with vertical federated learning. *arXiv preprint arXiv:2305.08328*.
- Wu, H., Zhao, Z., Chen, L.Y., Van Moorsel, A., 2022. Federated learning for tabular data: Exploring potential risk to privacy, in: 2022 IEEE 33rd International Symposium on Software Reliability Engineering (ISSRE), IEEE. pp. 193–204.
- Yang, Z., Wang, L., Yang, D., Wan, J., Zhao, Z., Chang, E.C., Zhang, F., Ren, K., 2023. Purifier: defending data inference attacks via transforming confidence scores, in: Proceedings of the AAAI Conference on Artificial Intelligence, pp. 10871–10879.
- Yeh, I.C., Lien, C.h., 2009. The comparisons of data mining techniques for the predictive accuracy of probability of default of credit card clients. *Expert systems with applications* 36, 2473–2480.
- Yin, Y., Zhang, X., Zhang, H., Li, F., Yu, Y., Cheng, X., Hu, P., 2023. Ginner: Generative model inversion attacks against collaborative inference, in: Proceedings of the ACM Web Conference 2023, pp. 2122–2131.
- Zeng, Y., Pan, M., Just, H.A., Lyu, L., Qiu, M., Jia, R., 2023. Narcissus: A practical clean-label backdoor attack with limited information, in: Proceedings of the 2023 ACM SIGSAC Conference on Computer and Communications Security, pp. 771–785.
- Zhao, B., Mopuri, K.R., Bilen, H., 2020. idlg: Improved deep leakage from gradients. *arXiv preprint arXiv:2001.02610*.
- Zhu, L., Liu, Z., Han, S., 2019. Deep leakage from gradients. *Advances in neural information processing systems* 32.
- Zhuang, W., Wen, Y., Zhang, S., 2021. Joint optimization in edge-cloud continuum for federated unsupervised person re-identification, in: Proceedings of the 29th ACM International Conference on Multimedia, pp. 433–441.